Mapping the developing human cardiac endothelium at single cell resolution identifies MECOM as a regulator of arteriovenous gene expression

CVR-2021-1517R2

Mapping the developing human cardiac endothelium at single cell resolution identifies MECOM as a regulator of arteriovenous gene expression

Authors:

Ian R. McCracken[1,2], Ross Dobie[3], Matthew Bennett[1], Rainha Passi[1], Abdelaziz Beqqali[1], Neil C. Henderson[3,4], Joanne C. Mountford[5], Paul R. Riley[2], Chris P. Ponting[4], Nicola Smart[2], Mairi Brittan[1], Andrew H. Baker[1,6*]

Affiliations:

[1]Centre for Cardiovascular Science, University of Edinburgh, Edinburgh EH16 4TJ, UK

[2]Department of Physiology, Anatomy, and Genetics, University of Oxford, Oxford OX1 3PT, UK

[3]Centre for Inflammation Research, University of Edinburgh, Edinburgh EH16 4TJ, UK

[4]MRC Human Genetics Unit, Institute of Genetics and Cancer, University of Edinburgh, Edinburgh EH4 2XU, UK

[5]Scottish National Blood Transfusion Service, Edinburgh EH14 4BE, UK

[6]Cardiovascular Research Institute Maastricht (CARIM), Maastricht University Medical Center, Maastricht, Netherlands

* Corresponding Author and Lead Contact: Andrew H. Baker, Centre for Cardiovascular Science, University of Edinburgh, 47 Little France Crescent, Edinburgh UK, EH16 4TJ, Tel: 0131 24 26728, Email: Andy.Baker@ed.ac.uk.

Total word count: 8948

Abstract

Aims: Coronary vasculature formation is a critical event during cardiac development, essential for heart function throughout perinatal and adult life. However, current understanding of coronary vascular development has largely been derived from transgenic mouse models. The aim of this study was to characterise the transcriptome of the human fetal cardiac endothelium using single-cell RNA sequencing (scRNA-seq) to provide critical new insights into the cellular heterogeneity and transcriptional dynamics that underpin endothelial specification within the vasculature of the developing heart.

Methods and Results: We acquired scRNA-seq data of over 10,000 fetal cardiac endothelial cells (EC), revealing divergent EC subtypes including endocardial, capillary, venous, arterial, and lymphatic populations. Gene regulatory network analyses predicted roles for *SMAD1* and *MECOM* in determining the identity of capillary and arterial populations, respectively. Trajectory inference analysis suggested an endocardial contribution to the coronary vasculature and subsequent arterialisation of capillary endothelium accompanied by increasing *MECOM* expression. Comparative analysis of equivalent data from murine cardiac development demonstrated that transcriptional signatures defining endothelial subpopulations are largely conserved between human and mouse. Comprehensive characterisation of the transcriptional response to MECOM knockdown in human embryonic stem cell-derived EC (hESC-EC) demonstrated an increase in the expression of non-arterial markers, including those enriched in venous EC.

Conclusions: scRNA-seq of the human fetal cardiac endothelium identified distinct EC populations. A predicted endocardial contribution to the developing coronary vasculature was identified, as well as subsequent arterial specification of capillary EC. Loss of *MECOM* in hESC-EC increased expression of non-arterial markers, suggesting a role in maintaining arterial EC identity.

Keywords: Human cardiac development, single-cell RNA sequencing, endothelial heterogeneity, coronary vasculature formation, MECOM, vascular regeneration.

Translational Perspective

Endogenous blood vessel formation in the adult heart following myocardial infarction is insufficient to support adequate survival of the remaining myocardium, often ultimately leading to heart failure. Improved understanding of the mechanisms regulating human coronary vessel formation is required to inform therapeutic strategies to reactivate developmental pathways promoting therapeutic angiogenesis in patients. We applied scRNA-seq to map the transcriptome of the endothelium of the developing human heart. We identified novel transcriptional signatures underlying the cellular heterogeneity and dynamic changes occurring within the developing cardiac endothelium. This included identifying and validating MECOM as a novel regulator of arterial EC identity which may serve as a target for therapeutic neovascularization.

1. Introduction

While the formation and homeostasis of the coronary vasculature is essential for heart muscle function, the molecular mechanisms underlying coronary vascular development remain incompletely understood. Previous studies using lineage tracing tools in mouse have provided much needed insight into these mechanisms, including identifying the endocardium and sinus venosus (SV) as the two major sources of coronary vascular endothelium during cardiac development[1, 2]. A third source, the proepicardium, was previously proposed to contribute a minor population of coronary endothelial cells (ECs)[3, 4], although this notion has recently been challenged[5]. Following the formation of the primitive coronary vascular plexus from these sources and onset of blood flow, subsequent remodelling occurs, giving rise to the distinct EC populations present in the mature vascular bed of the fully developed heart[6, 7]. Recent studies have elegantly mapped the remodelling of the immature coronary EC plexus in mouse cardiac development, including identification of a role for the transcription factor Dach1 in potentiating developmental arterial remodelling[7-9]. However, given that these advances in our understanding of coronary vascular development primarily originate from murine lineage tracing studies, the relevance of these findings for human cardiac development remains largely unknown.

Advances in single-cell RNA sequencing (scRNA-seq) have been instrumental in enhancing our understanding of embryonic development, permitting the objective mapping of underlying transcriptional changes at single-cell resolution. In addition, improvements in high throughput scRNA-seq platforms have facilitated the characterisation of tens of thousands of cells in parallel, thus allowing for ‘atlas’ studies to map the gene expression profile of entire organs during embryogenesis[10]. In recent years, such scRNA-seq studies have mapped the transcriptional profile of both murine and human heart development[11-19]. In

the study by Cui et al[13], scRNA-seq was conducted using cells isolated from specific regions of 18 human fetal hearts, ranging from 5 – 24 weeks gestation. Subsequent dimensionality reduction and clustering analysis revealed an EC cluster of 595 cells characterised by expression of endothelial markers such as *PECAM1*[13]. Similarly, a clear EC population was identified in a study from Suryawanshi et al[12] in which cells isolated from three healthy human fetal hearts (19-22 weeks) were processed using scRNA-seq. Both studies mapped the expression of known EC marker subtypes to allow annotation of clusters corresponding to endocardium, coronary vascular EC, and valvular EC. Nevertheless, the relatively low numbers of EC in these datasets prevented further characterisation of cardiac EC subtypes, including the identification of distinct arterial, venous, capillary, and lymphatic populations. In addition, these low EC numbers also prevented the application of methods to infer the dynamic cellular changes accompanying cardiac EC development.

While scRNA-seq studies of the developing mouse heart yielded large numbers of EC in their datasets[11, 16-18], their analysis focused on other cell types such as the cardiac conduction system, with minimal interpretation of EC heterogeneity and potential function. These included a study from Goodyer et al[15] which analysed distinct vascular EC and endocardial cell populations from E16.5 mouse hearts.

In this study we used scRNA-seq to comprehensively map the transcriptional signature of over 10,000 human fetal cardiac ECs isolated by fluorescence activated cell sorting (FACS) from two human fetal hearts at 13- and 14-weeks' gestation. Unsupervised clustering, gene regulatory analysis, and trajectory inference methods revealed the transcriptional profile of heterogeneous EC populations and predicted dynamic cellular changes including arterial EC specification. In addition, we functionally validated MECOM as a regulator of arterial EC

identity, thereby demonstrating the suitability of our novel scRNA-seq dataset to make *in silico* predictions, capable of informing future strategies to guide endothelial identity. Collectively, findings from this study complement and expand upon knowledge previously obtained from murine development, bringing insights into human EC heterogeneity and pathways determining specification of subpopulations that are essential for understanding human coronary vascular formation.

2. Methods

2.1 Tissue collection and study approval.

Human fetal cardiac tissue was acquired following elective termination of pregnancy. Informed written parental consent was obtained from all participants. Tissue was not collected in cases where termination of pregnancy was conducted due to an identified fetal or pregnancy abnormality. Ethical approval for the collection of fetal tissue was performed in accordance with all relevant guidelines and following study approval from the Lothian Research Ethics Committee (Study code: 08/1101/1) and the Research and Development Office (Study code: 2007/R/RM/10). This study was performed in accordance with the Declaration of Helsinki.

2.2 Isolation of fetal cardiac endothelial cells.

Cardiac endothelial cells were isolated from the ventricular tissue of freshly collected human fetal hearts using a method adapted from van Beijnum et al[20]. Digestion was performed at 37°C using a digestion solution containing 9ml 0.1% collagenase II and 1ml of 2.5U/ml dispase. 75µl of 1mg/ml DNaseI was added following 20 minutes incubation prior to a further 15 minutes incubation at 37°C. Digestion was quenched by the addition of 10ml cold RPMI with 10% FCS and undigested clumps of tissue removed using a 100µM cell strainer.

Red blood cell lysis was performed by incubating cells for 2 minutes in red blood cell lysis buffer at room temperature prior to neutralising with RPMI + 0.1% BSA. Cells were stained on ice for 45 minutes with APC anti-human CD31 and PE anti-human CD45 (Supplementary Table 1). CD31+ CD45- endothelial cells were isolated by fluorescence activated cell sorting (FACS) with DAPI staining being used to allow exclusion of dead cells.

2.3 Single-cell RNA sequencing of fetal cardiac endothelial cells.

Sorted CD31+ CD45- endothelial cells were counted manually using a haemocytometer with trypan blue staining used to identify non-viable cells. Viability exceeded 85% for both samples. 8,000 cells were loaded onto the 10X Chromium controller and library construction conducted using the Single Cell 3' Reagent Kit (V3.1) in accordance with the manufacturer's instructions. Libraries were sequenced using the Illumina NovaSeq 6000 platform.

2.4 Single-cell RNA sequencing data analysis.

Raw sequencing data was processed using the 10X CellRanger pipeline (Version 3.1.0.) aligning reads to the GRCh38-3.0.0 genome reference. Barcodes corresponding to cells were distinguished from those corresponding to empty droplets using both the DropUtils package[21] and the default cell calling method applied within the CellRanger pipeline. Cells with a total UMI count exceeding 3 median absolute deviations (MADs) from the median value were removed from downstream analysis using the R Scater package[22]. Similarly, cells with a high proportion of counts from mitochondrial genes (>3MADs) or with a low total gene count (<2 MADs) were also excluded. Data normalisation was performed using the MultiBatchNormalisation method[23] prior to merging datasets. Normalised count data was then scaled, and principal component analysis (PCA) applied using genes with the most variable expression across the combined dataset[24]. Following batch correction using

Harmony[25], non-supervised clustering was performed, and data visualised using Uniform Manifold Approximation and Projection (UMAP)[24]. A small cluster (155 cells) characterised by increased expression of fibroblast/ smooth muscle cell markers (*ACTA2* and *MYH11*) and reduced EC marker expression (*PECAM1* and *CDH5*) was removed from the dataset prior to rerunning data normalisation, PCA, and data visualisation. Significantly differentially expressed genes (DEGs) within individual clusters were identified using the Wilcoxon signed rank test (Bonferroni corrected p value <0.05) and a minimum $\log_e$(fold change) threshold of 0.3[24]. Additionally, only DEGs expressed in more than 30% of cells within their corresponding cluster were retained for further analysis.

Enriched metagene signatures were identified using the R package SCRAT v1.0.0[26]. Gene regulatory analysis was performed using the standard R SCENIC (Single Cell rEgulatory Network Inference and Clustering) workflow[27]. RNA velocity analysis was conducted using the python package scVelo[28] with the stochastic model being applied to predict the direction and magnitude of cellular dynamics. Trajectory inference tool Slingshot was performed using the standard workflow[29]. Genes significantly differentially expressed over pseudotime were identified using the TradeSeq package[30] with the top 2,000 most variably expressed genes in the dataset being used to fit the negative binomial generalised additive model (NB-GAM).

2.5 Human embryonic stem cell derived endothelial cell (hESC-EC) differentiation and siRNA mediated MECOM knockdown.

Human ESC lines were used in accordance with the UK Stem Cell Bank Steering Committee guidelines (Project Approvals SCS11-51 and SCSC17-26). H9 hESC were differentiated to hESC-EC as previously described[31, 32]. Small interfering RNA (siRNA) -mediated knockdown of MECOM was performed using day 7 hESC-EC using predesigned siRNA at a

final concentration of 5nM (Supplementary table 2). After 6 hours, transfection media was replaced with EGM-2 media supplemented with 1 % human AB serum and 50 ng/ml VEGF-A. At day 10, CD144+ hESC-EC were isolated by magnetic activated cell sorting (MACS) and cell pellets stored at -80°C for subsequent isolation of RNA and protein.

2.6 Bulk RNA sequencing analysis.

RNA was isolated from day 10 CD144+ hESC-EC previously subjected to either transfection with siRNA targeting MECOM (siRNA 1) or control siRNA (n=4 biological replicates). Illumina strand-specific RNA sequencing libraries with PolyA selection were prepared by GeneWiz (New Jersey, USA) and sequenced using the Illumina NovaSeq sequencer to achieve a read depth of 20 million paired end reads per sample.

Reads from each sample were mapped and quantified using RSEM[33] (v1.3.0, --bowtie2) and the GENCODE v38 primary assembly transcriptome. Genes with an average FPKM >1 in one or the other experimental group were considered to be expressed. To identify differentially expressed genes, tximport[34] (v1.22.0) was used to supply DESeq2[35] (v1.34.0) with the isoform read counts from RSEM before using the default DESeq2 method (Wald test) to obtain gene-level p values and fold changes between experimental conditions. Those genes with an absolute fold change value >1.5 (absolute Log2FC value > 0.584) and adjusted p value of <0.05 were considered differentially expressed. Over-represented KEGG terms amongst siMECOM-upregulated genes were identified using clusterProfiler[36] (v4.2.0) and Benjamini-Hochberg multiple hypothesis correction (p <0.05).

All further experimental and analysis details are included in the Supplementary Material Online Methods.

3. Results

3.1 Identification of distinct cardiac endothelial populations

Single-cell RNA sequencing (scRNA-seq) was performed on CD31+ CD45- cardiac endothelial cells isolated by FACS from ventricular tissue obtained from two human fetuses at 13 and 14 weeks of gestation (Figures 1A and 1B). At this developmental stage all major structures in the heart have formed, including the coronary vasculature. However, studies from equivalent timepoints in murine development (E15.5.-E17.5) have revealed extensive remodelling occurring within the established coronary vasculature producing a mature vascular bed containing heterogeneous EC populations[6, 9, 37]. Following quality control, unsupervised clustering, and UMAP visualisation of transcriptomic data from 10,267 cells, 11 distinct clusters (numbered 0-10) were revealed, each with expression of typical pan-endothelial cell (EC) markers (Figures 1C; Figure S1A). Leukocyte marker *PTPRC* and fibroblast/smooth muscle cell markers *ACTA2* and *MYH11* demonstrated negligible expression across all clusters (Figure S1A). Annotating cells by sample demonstrated successful integration of datasets, with each cluster containing cells from both samples (Figure S1B).

Expression of *NPR3*, a known endocardial marker, was localised to cluster 4 (Figure 1D; Figure S1C)[38]. Clusters 0, 1, 2, 5, and 6 were defined by expression of capillary marker *RGCC*[39], whilst arterial marker, *HEY1*[40], was expressed predominantly in clusters 2, 3, and 9 (Figure 1D; Figure S1C). Metagene analysis revealed 5 major signatures (A-E) indicating 5 key populations within the data (Figure 1E; Supplementary File 1). Signature A was enriched in clusters 2, 3, and 9, and included genes involved in arterial EC function such as *JAG1, DLL4,* and *HEY1* (Figure 1E). Furthermore, Gene Ontology (GO) term enrichment analysis

using signature A genes identified ‘artery morphogenesis’ and ‘positive regulation of Notch signalling pathway’ as significantly enriched terms (Figure 1F). Notch signalling is known to be required for arterial EC specification[41].

Signature B was predominantly enriched in cluster 4 and contained known endocardial markers *CDH11* and *NPR3* (Figure 1E and 1F)[38, 42]. Lower levels of signature B enrichment were also observed in clusters 7, 8, and 9 (Figure 1E). Clusters 0, 1, and 5 were enriched for signature C which included capillary EC marker genes such as *CA4* and *RGCC* (Figure 1E; Figure S1D)[39, 43]. Cluster 10 was enriched for signature D, for which GO term analysis returned terms relating to lymphatic EC (Figure 1E; Figure S1D). Lymphatic EC (LEC) markers[44], *LYVE1, FLT4, PROX1*, and *PDPN*, were differentially expressed in cluster 10 (Figure S1G). Signature E was selective for cluster 6 with GO term analysis identifying enriched terms relating to proliferation (Figure S1E). In line with this, categorising cells according to their predicted cell cycle phase revealed that 77 % of cells in cluster 6 were predicted to be in the G2M phase of rapid growth, whereas 95 % of cells in cluster 5 were in S phase (Figure S1F). The remaining cells in the dataset were predominantly in the G1 phase (79%), with only a small proportion predicted to be in G2M (4%) and S phases (17%) (Figure S1F). For clusters not associated with a metagene signature, analysis of differentially expressed genes (DEGs) revealed enrichment of *NR2F2* and *ACKR1* in cluster 7, suggesting a venous/venular EC identity (Figure 2A and S1G)[45, 46]. A valvular identity of cluster 8 was supported by its differential expression of *NFATC1* and *BMP4*, both with known roles in valvulogenesis (Fig S1G)[47, 48]. Collectively, these analyses demonstrate that each major subtype of EC within the heart (endocardial, venous, lymphatic, capillary, arterial, proliferating, and valvular EC) is represented by one or more of the identified 10 clusters.

3.2 Gene regulatory network analysis of fetal cardiac endothelial cells

Global differential gene expression analysis revealed markers for subpopulations of arterial and capillary cardiac EC (Figure 2A; Supplementary file 2). Notably, cluster 2, an arterial EC population, is more closely correlated with capillary EC clusters (0 and 1) than with the other two minor arterial clusters (3 and 9) (Figure S2A). Together with the co-expression of both arterial and capillary markers, this suggested that cluster 2 represents an arterial microvascular population. In contrast, arterial clusters 3 and 9 differentially expressed genes associated with ECM organisation (*FBLN5*, *ELN*, *FBN1*) and shear stress (*KLF4)* suggesting a macrovascular identity (Figures S2B and S2C).

Expression of fatty acid translocase encoding *CD36* was absent from macrovascular and endocardial populations, corresponding with a previous report of microvasculature-restricted expression (Figures 2A and 2B)[49]. Differential gene expression analysis revealed heterogeneity between the two major capillary clusters, 0 and 1. Cluster 0 was defined by differential expression of aminotransferase encoding gene, *INMT*, whilst *KIT* expression was enriched in cluster 1 (Figures 2A and 2B). Selective expression of *KIT* (also known as *C-KIT*) in cluster 1 was accompanied by upregulated expression of the transcription factor (TF) *SMAD1* (Figures S2D and S2E).

Gene regulatory network (GRN) analysis was applied to identify gene modules, known as regulons, predicted to be controlled by an individual TF, giving insight into the likely transcriptional regulators of EC heterogeneity. Visualisation of differentially expressed TFs and their predicted targets within the GRN largely recapitulated the data structure observed following unsupervised clustering (Figure 2C). Genes differentially expressed in LEC (cluster 10) localised together in the GRN and included TFs such as *PROX1*, a known master

regulator of LEC identity[50], as well as *HOXD9* and *TBX1* (Figure 2C). A set of differentially expressed endocardial TFs (cluster 4) was evident, including *GATA6, MEIS2*, and *FOXC1*, as well as *GATA4*, known to be implicated in endocardial cushion development[51, 52]. *MECOM* and *MAFF* were located amongst known regulators of arterial EC specification such as *HEY1* and *SOX17* (Figure 2C) [40, 53]. A distinct cluster of genes differentially expressed in *KIT1*$^{+}$ capillary EC (cluster 1) included *SOX4* and *SMAD1* (Figure 2C). Enrichment of *SOX4* and *SMAD1* regulons was also observed in *KIT1+* capillary EC (Figure 2D).

3.3 Trajectory analysis predicts an endocardial contribution to the developing coronary vasculature and potential regulators of subsequent arterial specification

Several recent studies using murine models of coronary vascular development have provided insight into the origin of the coronary endothelium and the dynamic changes that occur during its subsequent remodelling[6, 54]. Endocardial derived vessels vascularise the heart from the inside-out contributing to vessels of the interventricular septum and inner myocardial wall[1, 55, 56]. Conversely, sinus venosus (SV) derived vessels populate the outer ventricular free walls of the heart from the outside-in[38, 55, 56]. Following the formation of the primitive coronary vascular plexus, EC undergo further remodelling to form a functional network of veins, arteries, and capillaries[9].

We used trajectory inference methods to determine whether these processes could be identified during human cardiac development and to characterise their accompanying transcriptional changes. Given that these dynamic changes are known to originate from microvascular EC, we excluded the two previously identified arterial macrovascular clusters (clusters 3 and 9) from the dataset and performed secondary clustering of the remaining cells (Figure 3A). The distinct LEC cluster was also excluded prior to re-clustering. The same

marker genes used for annotating the complete dataset were used for the annotation of re-clustered data (Figure S3A).

RNA velocity analysis[28], which utilises the ratio of spliced to unspliced transcripts to infer the direction and magnitude of cellular transitions, was first used to gain an overview of the pseudotemporal dynamics of the fetal cardiac endothelium (Figures 3A and S3B). We identified a proportion of the endocardial cluster with velocity vectors indicating a probable transition towards a venous identity (Figure 3A and S3B). Evidence for this transition was further supported by venous EC associated genes such as *PLVAP* and *NR2F2*, having positive residuals/velocities in endocardial cells (Figure S3C). In turn, venous EC were subsequently predicted to transition to *INMT*+ capillary EC. This predicted transition of endocardium to coronary vascular EC concurs with studies that identified the endocardium as a significant source of EC for the coronary vasculature. To further substantiate this finding, cells belonging to endocardial, venous, and *INMT*+ capillary clusters were isolated *in silico* and reclustered. UMAP visualisation of reclustered data revealed a comparable result to previous analysis with endocardial and *INMT*+ capillary populations connected by a *ACKR1*+ venous population (Figure S3D). Additionally, the omission of cell cycle related genes from clustering and visualisation calculations generated a comparable finding, thus confirming localisation of identified clusters was not confounded by cell cycle related effects (Figure S3E). Velocity analysis also predicted a likely transition of both capillary EC populations towards an arterial EC fate (Figures 3A and S3B). This is an agreement with previous reports of developmental arterial remodelling in mouse[7-9].

In addition to the RNA velocity analysis, we also independently applied the trajectory inference tool Slingshot[29], which yielded a comparable interpretation (Figure 3B).

Identification of the top 200 genes with most variable expression over pseudotime revealed 4 temporal patterns of expression, arranged in modules 1 - 4 (Figures 3C and 3D). Average sample module gene expression was visualised over pseudotime to ensure concordant expression dynamics between individual samples. Module 2 genes were expressed early in pseudotime with their reduction in expression occurring in conjunction with the loss of endocardial identity (Figure 3D). These included known markers of endocardium such as *CDH11* and *NPR3* as well as the TFs *DKK3* and *GATA6* (Figure 3E and S4A). TFs *CEBPD* and *FOS* were identified in module 1 along with *NR2F2*, a known regulator of venous EC specification[45] (Figure S4A). Interestingly, despite not being identified within module 1, expression of *BMP2* was found to increase within the pseudotime range corresponding to the predicted transitioning venous population (Figure S4B). As well as demonstrating enriched expression in venous EC in zebrafish[57], BMP2 has also recently been identified as positive regulator of endocardial to coronary vascular EC transition during murine cardiac development[58]. Module 4 genes demonstrated peak expression within *IMNT*+ capillary EC and included TFs *TCF15* and *MEOX1* (Figure 3E). Expression of *DACH1* was found to peak within the *IMNT*$^{+}$ capillary cluster before gradually decreasing again within the arterial population (Figure S4C). Previous studies have identified *Dach1* as a driver of developmental arterial remodelling in murine cardiac development[8, 9].

The predicted transition of capillary EC to arterial EC was defined by increased expression of module 3 genes (Figures 3C-D). This included *HEY1*, known to mediate arterial EC specification[40]. Interestingly, module 3 also contained the TF *MECOM*, earlier predicted by GRN analysis to underlie arterial EC identity (Figures 2C and 3C-E; Figure S4A). Subsequent in situ hybridisation (ISH) validation conducted across four independent fetal hearts (aged 13-14 weeks) demonstrated clear coexpression of *MECOM* with the arterial EC

enriched TF *HEY1* within arterial vessels (Figure 3F and S5A-B). Notably, a lack of *MECOM* expression was observed in vessels with venous morphology validating its arterial EC specificity (Figure 3F and S5A-B). In addition, reanalysis of publicly available scRNA-seq data from healthy human fetal heart data from Surywanshi et al[12] revealed *MECOM* expression to be enriched within a subset of the endocardial/endothelial population with minimal expression in other identified cell types (Figure S6A-C).

3.4 Comparison with murine coronary developmental gene expression reveals conserved markers of cardiac endothelial cell populations

Our current understanding of cardiac vascular development is derived predominantly from murine models. Consequently, we next compared the transcriptional profiles of developing fetal human and embryonic mouse cardiac EC. For this comparison, a publicly available mouse embryonic heart scRNA-seq dataset[15] was used due to its good representation of cardiac EC and because its embryonic stage (E16.5) corresponded with the later developmental stage of our human fetal heart data (13-14 weeks)[37].

Dimensionality reduction revealed successful integration of mouse and human cardiac EC (Figure S7A). Unlike our observation in the human heart, no distinct populations of *KIT*+ or *INMT*+ capillary populations were observed in the mouse data (Figure S7B). Clusters were therefore merged to represent the major subtypes of EC within the heart (endocardial, venous, lymphatic, capillary, arterial, proliferating, and valvular EC). Genes found to be amongst the most significantly differentially expressed in the same population in both human and mouse were classified as conserved markers (Figure 4A). *MECOM* and *UNC5B* were among genes with enriched arterial EC expression in both species (Figures 4A-B). In agreement with previous findings in mouse[38], *NPR3* expression was highly specific to the endocardial

population with minimal expression in valvular EC[38]. A lack of clear conserved venous EC markers was observed, with partial overlap of DEG in some lymphatic, valvular, and endocardial populations (Figures 4A-B). Interestingly, whilst the known LEC TF, *PROX1*, was expressed in both valvular EC and LEC in both species, *PTX3* and a LEC marker, *LYVE1*, were found to be highly LEC specific (Figures 4A-B). Species-specific markers were also identified for each EC dataset (Figures 4A and S7C). A human endocardial marker, *NPCC*, described elsewhere as specifically defining human fetal cardiac endocardium[12], was not enriched in the corresponding mouse population (Figure 4C).

3.5 MECOM is required in arterial-like hESC-EC to suppress non-arterial gene expression

Given the *in-silico* predictions of a role for *MECOM* in arterial fate and enriched *MECOM* expression in arterial EC for both human and mouse, suggesting an evolutionarily conserved role in arterial EC, we sought to validate its role in determining human arterial EC identity. Our previous scRNA-seq based characterisation of our 8 day hESC-EC differentiation protocol demonstrated its suitability as an *in vitro* model of human EC development[32]. Additionally, we determined that after acquisition of an early EC identity by day 6, hESC-EC assume a clear arterial-like EC transcriptional signature by day 8, characterised by expression of arterial markers such as *SOX17* and *DLL4* (Figure S8A). Expression of venous (*NR2F2, EPHB4*) and lymphatic markers (*PROX1*) in hESC-EC was low by day 8 of the differentiation (Figure S8A). Notably, in agreement with its arterial EC specificity, *MECOM* was specifically expressed in hESC-EC at days 6 and 8 of differentiation (Figure S8A).

Using hESC-EC as a developmental model for arterial EC specification, we next determined whether small interfering RNA (siRNA)-mediated MECOM knockdown in hESC-EC

resulted in changes to their arteriovenous identity (Figure 5A). Significant knockdown (>50%) of MECOM was observed at the RNA and protein level in hESC-EC 72 hours after siRNA transfection (Figures 5B and S8B-C). Bulk RNA sequencing analysis revealed a distinct transcriptional profile for hESC-EC following MECOM knockdown compared to that of control hESC-EC (Figure S8D). Differential gene expression analysis demonstrated a reduction of MECOM resulted in a global increase in expression of non-arterial markers, including *NR2F2*[45] ($Log_2FC = 1.89$) and *VWF*[59] ($Log_2FC = 0.95$) known to be enriched in venous EC (Figure 5C; Supplementary file 3). Notably, known arterial markers including *HEY1* and *DLL4* were found not to be significantly downregulated in response to MECOM knockdown. In addition to the upregulation of known venous markers, several genes with previously reported differential expression in LEC including *LYVE1*[44] ($Log_2FC = 1.29$), *STAB2*[60] ($Log_2FC = 4.05$), and *CEACAM1*[61] ($Log_2FC = 1.74$) were also found to be significantly upregulated (Figure 5C). However, expression of key LEC TF *PROX1* was not detected in either condition.

Application of an upregulated gene expression signature (constructed using the top 20 upregulated genes following MECOM KD in hESC-EC) to our fetal cardiac EC scRNA-seq dataset revealed the lowest level of signature enrichment in arterial populations, with highest levels of enrichment observed in lymphatic and venous clusters (Figure 5D). KEGG pathway enrichment analysis conducted using genes significantly upregulated following MECOM KD identified enrichment of genes belonging to the PI3K-AKT signalling pathway, reported to play a role in venous EC specification[62, 63] (Figure 5E). qRT-PCR validation aligned with bulk RNA seq findings demonstrating knockdown of MECOM resulted in significant upregulation of venous EC markers (*NR2F2* and *EPHB4*) whilst arterial (*HEY1*, *DLL4*, *JAG1*, *JAG2*) markers remained unchanged (Figure 5F; Figure S8E). Importantly, reduction

of MECOM did not result in altered expression of the pan-endothelial marker, *CDH5*, suggesting that the changes observed in arteriovenous marker expression are not due to a loss of general EC identity (Figure S8E).

4. Discussion

In this study we comprehensively mapped the transcriptional landscape of the developing human fetal heart endothelium using scRNA-seq. Isolation of fetal cardiac EC by FACS prior to performing high throughput scRNA-seq empowered this study to identify the full extent of EC heterogeneity. This included identifying distinct endocardial, valvular, venous, capillary, and arterial EC populations each expressing a separate transcriptional signature.

Gene regulatory network analysis identified the TFs most likely responsible for establishing the observed endothelial cell heterogeneity. Application of trajectory inference methods to microvascular ECs was used to map the cellular dynamics accompanying coronary vascular EC development. This revealed a small proportion of endocardial cells that appeared to transition to a vascular EC identity *via* a venous EC population. In addition, capillary EC were predicted to be undergoing specification to assume an arterial EC identity, defined by increasing expression of the TF, *MECOM*. Comparison of our human fetal heart EC data with E16.5 murine cardiac EC scRNA-seq data demonstrated the existence of several conserved, as well as species-specific, markers for each of the major cardiac EC populations. This included identifying *NPR3* and *MECOM* as conserved markers of endocardial and arterial populations, respectively. Finally, we demonstrated that loss of MECOM in arterial-like hESC-EC resulted in a global increased expression of non-arterial markers, suggesting a function to maintain identity in arterial EC.

In contrast to the capillary EC cluster defined by differential expression of methyltransferase encoding gene, *INMT*, gene regulatory network analysis revealed several regulons enriched within the *KIT*+ capillary population. This included the *SMAD1* regulon. BMP/SMAD1 signalling has been demonstrated to promote angiogenesis whilst KIT/C-KIT has been shown to mediate neovascularisation in retinal microvascular endothelial cells in response to hypoxia[64, 65]. This suggests that *SMAD1* may mediate angiogenesis within hypoxic regions in the developing heart wall, although this will require further investigation to verify. The existence of two capillary populations with distinct transcriptional signatures, including the differential expression of *KIT* and *INMT*, was recently confirmed in an independent study from Phansalkar et al[19] which performed low throughput scRNA-seq on EC isolated from 11-, 14- and 22-week human fetal hearts.

Our *in-silico* findings suggested a transition of endocardium to coronary vascular endothelium. This is consistent with previous findings from murine lineage-tracing studies, in which a proportion of the endocardium gives rise to coronary vascular EC *via* angiogenic sprouting[1]. A second method of endocardial derived coronary vessel formation during was also proposed to occur at the murine perintal stage and involve the formation of new coronary vessels by the segregation of endocardial trabeculae protruding into the myocardium during compaction[66]. However, this model has recently been challenged by Lu et al[67] which concluded that formation of new coronary vessels during the perinatal stage is instead due to angiogenic expansion of the pre-existing coronary plexus.

Although our trajectory analysis indicated the transition of endocardium to coronary vasculature occurs *via* a venous EC population, the arteriovenous identity of cells undergoing this process has not previously been explored. Whilst studies in mouse have demonstrated a

significant proportion of coronary vascular EC to be derived from venous cells of the SV, this is thought to occur much earlier in cardiac development than the comparative gestational age of the human fetal samples used in this analysis[2, 38]. However, the observed enrichment of *BMP2* expression within the identified venous cluster aligns closely with recent scRNA-seq evidence from D'Amato et al identifying *Bmp2* as a marker of the transitioning endocardial population in E12 mouse embryos[58]. Additionally, enriched venous expression of bmp2 has previously been described in zebrafish[57], thus further indicating the identified venous cluster may represent a transitioning endocardial-derived population.

Trajectory inference analysis also revealed subsequent arterial specification of capillary EC. This predicted cellular transition in the human fetal heart was also recently identified by Phansalkar el al[19], thus collectively providing human relevance to current understanding of coronary artery development derived from murine studies[7-9]. However, in addition to confirming the upregulation of known mediators of arterial specification such as *HEY1*[40] and *SOX17*[53], *MECOM* was also identified as having a role in the establishment of an arterial EC identity. Furthermore, enriched arterial expression of MECOM was also observed in coronary EC from E16.5 mouse hearts, suggesting an evolutionarily conserved function.

The localisation of *MECOM* in the developing human heart was validated using ISH methods and its function in arterial EC identity demonstrated by siRNA mediated knockdown in arterial-like hESC-EC. Previous work from Li et al[68] demonstrated that MECOM acts upstream of Notch signalling during zebrafish nephrogenesis. Given the importance of Notch signalling in arterial EC specification, this suggested that MECOM may alter arteriovenous identity by regulating Notch signalling. Whilst reduction in MECOM expression in hESC-EC did not alter the expression of arterial EC markers, including those belonging to the Notch

pathway, a global increase in the expression of non-arterial enriched genes was observed. This included the TF, *NR2F2*, which is known to establish venous identity, in part *via* repression of Notch signalling[45]. Although a subset of genes upregulated following MECOM knockdown have been reported to be differentially expressed in LEC, the absence of increased *PROX1* expression indicated the reduction in MECOM does not specify EC towards a lymphatic identity.

Collectively, these findings suggest that MECOM may be required to supress non-arterial gene expression during arterial EC specification. Goyama et al[69] previously demonstrated that loss of MECOM within Tie2+ cells results in severe vascular abnormalities leading to embryonic lethality in mouse between E13.5 and E16.5. However, considering our described findings, further investigation is required to characterise *MECOM* expression across the murine embryonic and adult coronary vascular endothelium, as well as to evaluate the resultant effect of EC specific loss of MECOM on arteriovenous identity.

Previous studies from mouse have hypothesised that a venous identity is the default state for EC, with venous identity needing to be repressed via Notch signalling during arterial specification[70, 71]. Our finding that MECOM knockdown altered venous marker (*NR2F2* and *EPHB4*) expression, without changes to expression of Notch signalling genes, suggests that additional factors are required to supress venous identity during human arterial EC specification. However, further studies simultaneously targeting the expression of characterised arterial EC regulators is required to determine the position of MECOM within the hierarchal network of arteriovenous regulators. Previous findings in mouse demonstrated overexpression of arterial EC regulator Dach1 resulted in an increase in perfused arteries following myocardial infarction[8]. Our finding from human data suggesting MECOM may

function to maintain the transcriptional identity of arterial EC highlights it as a prime therapeutic candidate to drive arterialisation in cardiovascular disease.

Although this study is the most comprehensive of its type to date, due to limited sample availability its data provides only a snapshot of a narrow developmental window (13-14 weeks). This limitation prevented the comparison of gene expression and cluster proportion between different gestational ages. Careful batch correction and visualisation of gene expression dynamics across pseudotime for individual samples ensured findings from trajectory inference analysis were not biased by unequal representation of individual clusters. Whilst trajectory inference methods permit the dynamical changes to be characterised within individual datasets, inclusion of fetal samples from a wider range of gestational ages would provide a more comprehensive understanding of human coronary vascular development, especially at earlier stages.

In summary, we have used a high throughput scRNA-seq platform to comprehensively map the transcriptional landscape of the human fetal heart endothelium at 13-14 weeks. This study complements studies using murine models of cardiovascular development by providing novel insight into endothelial cell heterogeneity within the developing human heart, as well as the dynamical changes accompanying coronary vasculature formation. In addition to helping understand the mechanisms giving rise to congenital coronary vascular abnormalities, this information may prove valuable in future strategies to guide coronary vascular formation for the treatment of coronary vascular disease.

Funding

This work was supported by Medical Research Council [MRC Precision Medicine Doctoral Training Programme to I.R.M. and MRC program: Computational and Disease Genomics (MC_UU_00007/15) to C.P.P.], Wellcome Trust [Wellcome Trust Senior Research Fellowship in Clinical Science (ref. 219542/Z/19/Z) to N.C.H.], British Heart Foundation [Personal Chair Award (#CH/11/1/28798) to P.R.R. , Intermediate Basic Science Research Fellowship (FS/16/4/31831) to M.B., BHF Chair (CH/11/2/28733), BHF Programme grant (RG/20/5/34796), and Centre for Regenerative Medicine (CRMR/21/290009) to A.H.B.], Chief Scientists Office [CSO grant (CGA/19/18) to A.H.B.], and the ERC [Advanced Grant VASCMIR (338991) to A.H.B].

Author Contributions

I.R.M., J.C.M., N.S., M.B. and A.H.B. were involved in the design of the described study. I.R.M. and R.D. carried out fetal tissue collection and sample processing. Bioinformatic analysis was performed by I.R.M. and M.B. In vitro experiments, qRT-PCR, and western blotting analysis was conducted by I.R.M., R.P., and A.B. A.H.B., C.P.P. and M.B. supervised the research. A.H.B. secured research funding. I.R.M., M.B., N.C.H., J.C.M., P.R.R., C.P.P., N.S., M.B., and A.H.B. were involved in interpreting bioinformatics data. I.R.M. and A.H.B wrote the manuscript with input from all authors. All authors discussed the data and edited the manuscript.

Acknowledgements

The authors thank Andrea Corsinotti for his assistance in generating 10X scRNA-seq libraries and Kathryn Newton for her technical support. FACS was performed with support from both the CRM Flow and Genomic Cytometry Core Facility and the QMRI Flow Cytometry and cell

sorting facility, University of Edinburgh. For in situ hybridisation validations, human embryonic and fetal material was provided by the Joint MRC / Wellcome Trust (Grant # MR/006237/1) Human Developmental Biology Resource (http://www.hdbr.org) and performed by the HDBR in house gene expression service.

Conflict of interest: none declared.

Data availability

RNA sequencing data used in this study is accessible from the Gene Expression Omnibus (accession number: GSE195911).

References

1. Wu B, Zhang Z, Lui W, Chen X, Wang Y, Chamberlain AA, Moreno-Rodriguez Ricardo A, Markwald Roger R, O'Rourke Brian P, Sharp David J, Zheng D, Lenz J, Baldwin HS, Chang C-P, Zhou B. Endocardial Cells Form the Coronary Arteries by Angiogenesis through Myocardial-Endocardial VEGF Signaling. *Cell* 2012;**151**:1083-1096.
2. Red-Horse K, Ueno H, Weissman IL, Krasnow MA. Coronary arteries form by developmental reprogramming of venous cells. *Nature* 2010;**464**:549-553.
3. Cai C-L, Martin JC, Sun Y, Cui L, Wang L, Ouyang K, Yang L, Bu L, Liang X, Zhang X, Stallcup WB, Denton CP, McCulloch A, Chen J, Evans SM. A myocardial lineage derives from Tbx18 epicardial cells. *Nature* 2008;**454**:104-108.
4. Katz TC, Singh MK, Degenhardt K, Rivera-Feliciano J, Johnson RL, Epstein JA, Tabin CJ. Distinct compartments of the proepicardial organ give rise to coronary vascular endothelial cells. *Dev Cell* 2012;**22**:639-650.
5. Lupu IE, Redpath AN, Smart N. Spatiotemporal Analysis Reveals Overlap of Key Proepicardial Markers in the Developing Murine Heart. *Stem Cell Reports* 2020;**14**:770-787.
6. Sharma B, Chang A, Red-Horse K. Coronary Artery Development: Progenitor Cells and Differentiation Pathways. *Annu Rev Physiol* 2017;**79**:1-19.
7. Su T, Stanley G, Sinha R, D'Amato G, Das S, Rhee S, Chang AH, Poduri A, Raftrey B, Dinh TT, Roper WA, Li G, Quinn KE, Caron KM, Wu S, Miquerol L, Butcher EC, Weissman I, Quake S, Red-Horse K. Single-cell analysis of early progenitor cells that build coronary arteries. *Nature* 2018;**559**:356-362.
8. Raftrey B, Williams I, Rios Coronado PE, Fan X, Chang AH, Zhao M, Roth R, Trimm E, Racelis R, D'Amato G, Phansalkar R, Nguyen A, Chai T, Gonzalez KM, Zhang Y, Ang LT, Loh KM, Bernstein D, Red-Horse K. Dach1 Extends Artery Networks and Protects Against Cardiac Injury. *Circ Res* 2021;**129**:702-716.
9. Chang AH, Raftrey BC, D'Amato G, Surya VN, Poduri A, Chen HI, Goldstone AB, Woo J, Fuller GG, Dunn AR, Red-Horse K. DACH1 stimulates shear stress-guided endothelial cell migration and coronary artery growth through the CXCL12-CXCR4 signaling axis. *Genes Dev* 2017;**31**:1308-1324.
10. Potter SS. Single-cell RNA sequencing for the study of development, physiology and disease. *Nat Rev Nephrol* 2018;**14**:479-492.
11. DeLaughter DM, Bick AG, Wakimoto H, McKean D, Gorham JM, Kathiriya IS, Hinson JT, Homsy J, Gray J, Pu W, Bruneau BG, Seidman JG, Seidman CE. Single-Cell Resolution of Temporal Gene Expression during Heart Development. *Dev Cell* 2016;**39**:480-490.
12. Suryawanshi H, Clancy R, Morozov P, Halushka MK, Buyon JP, Tuschl T. Cell atlas of the foetal human heart and implications for autoimmune-mediated congenital heart block. *Cardiovasc Res* 2020;**116**:1446-1457.
13. Cui Y, Zheng Y, Liu X, Yan L, Fan X, Yong J, Hu Y, Dong J, Li Q, Wu X, Gao S, Li J, Wen L, Qiao J, Tang F. Single-Cell Transcriptome Analysis Maps the Developmental Track of the Human Heart. *Cell Rep* 2019;**26**:1934-1950.e1935.
14. Asp M, Giacomello S, Larsson L, Wu C, Fürth D, Qian X, Wärdell E, Custodio J, Reimegård J, Salmén F, Österholm C, Ståhl PL, Sundström E, Åkesson E, Bergmann O, Bienko M, Månsson-Broberg A, Nilsson M, Sylvén C, Lundeberg J. A Spatiotemporal Organ-Wide Gene Expression and Cell Atlas of the Developing Human Heart. *Cell* 2019;**179**:1647-1660.e1619.

15. Goodyer WR, Beyersdorf BM, Paik DT, Tian L, Li G, Buikema JW, Chirikian O, Choi S, Venkatraman S, Adams EL, Tessier-Lavigne M, Wu JC, Wu SM. Transcriptomic Profiling of the Developing Cardiac Conduction System at Single-Cell Resolution. *Circ Res* 2019;**125**:379-397.
16. Li G, Tian L, Goodyer W, Kort EJ, Buikema JW, Xu A, Wu JC, Jovinge S, Wu SM. Single cell expression analysis reveals anatomical and cell cycle-dependent transcriptional shifts during heart development. *Development* 2019;**146**.
17. Li G, Xu A, Sim S, Priest JR, Tian X, Khan T, Quertermous T, Zhou B, Tsao PS, Quake SR, Wu SM. Transcriptomic Profiling Maps Anatomically Patterned Subpopulations among Single Embryonic Cardiac Cells. *Dev Cell* 2016;**39**:491-507.
18. de Soysa TY, Ranade SS, Okawa S, Ravichandran S, Huang Y, Salunga HT, Schricker A, Del Sol A, Gifford CA, Srivastava D. Single-cell analysis of cardiogenesis reveals basis for organ-level developmental defects. *Nature* 2019;**572**:120-124.
19. Phansalkar R, Krieger J, Zhao M, Kolluru SS, Jones RC, Quake SR, Weissman I, Bernstein D, Winn VD, D'Amato G, Red-Horse K. Coronary blood vessels from distinct origins converge to equivalent states during mouse and human development. *Elife* 2021;**10**.
20. van Beijnum JR, Rousch M, Castermans K, van der Linden E, Griffioen AW. Isolation of endothelial cells from fresh tissues. *Nat Protoc* 2008;**3**:1085-1091.
21. Lun ATL, Riesenfeld S, Andrews T, Dao TP, Gomes T, Marioni JC, participants in the 1st Human Cell Atlas J. EmptyDrops: distinguishing cells from empty droplets in droplet-based single-cell RNA sequencing data. *Genome Biology* 2019;**20**:63.
22. McCarthy DJ, Campbell KR, Lun ATL, Wills QF. Scater: pre-processing, quality control, normalization and visualization of single-cell RNA-seq data in R. *Bioinformatics* 2017;**33**:1179-1186.
23. Haghverdi L, Lun ATL, Morgan MD, Marioni JC. Batch effects in single-cell RNA-sequencing data are corrected by matching mutual nearest neighbors. *Nature Biotechnology* 2018;**36**:421-427.
24. Stuart T, Butler A, Hoffman P, Hafemeister C, Papalexi E, Mauck WM, III, Hao Y, Stoeckius M, Smibert P, Satija R. Comprehensive Integration of Single-Cell Data. *Cell* 2019;**177**:1888-1902.e1821.
25. Korsunsky I, Millard N, Fan J, Slowikowski K, Zhang F, Wei K, Baglaenko Y, Brenner M, Loh P-r, Raychaudhuri S. Fast, sensitive and accurate integration of single-cell data with Harmony. *Nature Methods* 2019;**16**:1289-1296.
26. Camp JG, Sekine K, Gerber T, Loeffler-Wirth H, Binder H, Gac M, Kanton S, Kageyama J, Damm G, Seehofer D, Belicova L, Bickle M, Barsacchi R, Okuda R, Yoshizawa E, Kimura M, Ayabe H, Taniguchi H, Takebe T, Treutlein B. Multilineage communication regulates human liver bud development from pluripotency. Nature. England, 2017:533-538.
27. Aibar S, Gonzalez-Blas CB, Moerman T, Huynh-Thu VA, Imrichova H, Hulselmans G, Rambow F, Marine JC, Geurts P, Aerts J, van den Oord J, Atak ZK, Wouters J, Aerts S. SCENIC: single-cell regulatory network inference and clustering. *Nat Methods* 2017;**14**:1083-1086.
28. Bergen V, Lange M, Peidli S, Wolf FA, Theis FJ. Generalizing RNA velocity to transient cell states through dynamical modeling. *Nature Biotechnology* 2020;**38**:1408-1414.
29. Street K, Risso D, Fletcher RB, Das D, Ngai J, Yosef N, Purdom E, Dudoit S. Slingshot: cell lineage and pseudotime inference for single-cell transcriptomics. *BMC Genomics* 2018;**19**:477.

30. Van den Berge K, Roux de Bézieux H, Street K, Saelens W, Cannoodt R, Saeys Y, Dudoit S, Clement L. Trajectory-based differential expression analysis for single-cell sequencing data. *Nature Communications* 2020;**11**:1201.
31. MacAskill MG, Saif J, Condie A, Jansen MA, MacGillivray TJ, Tavares AAS, Fleisinger L, Spencer HL, Besnier M, Martin E, Biglino G, Newby DE, Hadoke PWF, Mountford JC, Emanueli C, Baker AH. Robust Revascularization in Models of Limb Ischemia Using a Clinically Translatable Human Stem Cell-Derived Endothelial Cell Product. *Mol Ther* 2018;**26**:1669-1684.
32. McCracken IR, Taylor RS, Kok FO, de la Cuesta F, Dobie R, Henderson BEP, Mountford JC, Caudrillier A, Henderson NC, Ponting CP, Baker AH. Transcriptional dynamics of pluripotent stem cell-derived endothelial cell differentiation revealed by single-cell RNA sequencing. *European Heart Journal* 2020;**41**:1024-1036.
33. Li B, Dewey CN. RSEM: accurate transcript quantification from RNA-Seq data with or without a reference genome. *BMC Bioinformatics* 2011;**12**:323.
34. Soneson C, Love MI, Robinson MD. Differential analyses for RNA-seq: transcript-level estimates improve gene-level inferences. *F1000Res* 2015;**4**:1521.
35. Love MI, Huber W, Anders S. Moderated estimation of fold change and dispersion for RNA-seq data with DESeq2. *Genome Biol* 2014;**15**:550.
36. Wu T, Hu E, Xu S, Chen M, Guo P, Dai Z, Feng T, Zhou L, Tang W, Zhan L, Fu X, Liu S, Bo X, Yu G. clusterProfiler 4.0: A universal enrichment tool for interpreting omics data. *Innovation (N Y)* 2021;**2**:100141.
37. Krishnan A, Samtani R, Dhanantwari P, Lee E, Yamada S, Shiota K, Donofrio MT, Leatherbury L, Lo CW. A detailed comparison of mouse and human cardiac development. *Pediatr Res* 2014;**76**:500-507.
38. Zhang H, Pu W, Li G, Huang X, He L, Tian X, Liu Q, Zhang L, Wu SM, Sucov HM, Zhou B. Endocardium Minimally Contributes to Coronary Endothelium in the Embryonic Ventricular Free Walls. *Circ Res* 2016;**118**:1880-1893.
39. Kalucka J, de Rooij LPMH, Goveia J, Rohlenova K, Dumas SJ, Meta E, Conchinha NV, Taverna F, Teuwen L-A, Veys K, García-Caballero M, Khan S, Geldhof V, Sokol L, Chen R, Treps L, Borri M, de Zeeuw P, Dubois C, Karakach TK, Falkenberg KD, Parys M, Yin X, Vinckier S, Du Y, Fenton RA, Schoonjans L, Dewerchin M, Eelen G, Thienpont B, Lin L, Bolund L, Li X, Luo Y, Carmeliet P. Single-Cell Transcriptome Atlas of Murine Endothelial Cells. *Cell* 2020;**180**:764-779.e720.
40. Fischer A, Schumacher N, Maier M, Sendtner M, Gessler M. The Notch target genes Hey1 and Hey2 are required for embryonic vascular development. *Genes Dev* 2004;**18**:901-911.
41. Kume T. Specification of arterial, venous, and lymphatic endothelial cells during embryonic development. *Histol Histopathol* 2010;**25**:637-646.
42. Zhou J, Bowen C, Lu G, Knapp Iii C, Recknagel A, Norris RA, Butcher JT. Cadherin-11 expression patterns in heart valves associate with key functions during embryonic cushion formation, valve maturation and calcification. *Cells Tissues Organs* 2013;**198**:300-310.
43. Gillich A, Zhang F, Farmer CG, Travaglini KJ, Tan SY, Gu M, Zhou B, Feinstein JA, Krasnow MA, Metzger RJ. Capillary cell-type specialization in the alveolus. *Nature* 2020;**586**:785-789.
44. Oliver G, Kipnis J, Randolph GJ, Harvey NL. The Lymphatic Vasculature in the 21(st) Century: Novel Functional Roles in Homeostasis and Disease. *Cell* 2020;**182**:270-296.

45. You L-R, Lin F-J, Lee CT, DeMayo FJ, Tsai M-J, Tsai SY. Suppression of Notch signalling by the COUP-TFII transcription factor regulates vein identity. *Nature* 2005;**435**:98-104.
46. Thiriot A, Perdomo C, Cheng G, Novitzky-Basso I, McArdle S, Kishimoto JK, Barreiro O, Mazo I, Triboulet R, Ley K, Rot A, von Andrian UH. Differential DARC/ACKR1 expression distinguishes venular from non-venular endothelial cells in murine tissues. *BMC Biol* 2017;**15**:45.
47. Wu B, Wang Y, Lui W, Langworthy M, Tompkins KL, Hatzopoulos AK, Baldwin HS, Zhou B. Nfatc1 coordinates valve endocardial cell lineage development required for heart valve formation. *Circ Res* 2011;**109**:183-192.
48. McCulley DJ, Kang JO, Martin JF, Black BL. BMP4 is required in the anterior heart field and its derivatives for endocardial cushion remodeling, outflow tract septation, and semilunar valve development. *Dev Dyn* 2008;**237**:3200-3209.
49. Son NH, Basu D, Samovski D, Pietka TA, Peche VS, Willecke F, Fang X, Yu SQ, Scerbo D, Chang HR, Sun F, Bagdasarov S, Drosatos K, Yeh ST, Mullick AE, Shoghi KI, Gumaste N, Kim K, Huggins LA, Lhakhang T, Abumrad NA, Goldberg IJ. Endothelial cell CD36 optimizes tissue fatty acid uptake. *J Clin Invest* 2018;**128**:4329-4342.
50. Wigle JT, Harvey N, Detmar M, Lagutina I, Grosveld G, Gunn MD, Jackson DG, Oliver G. An essential role for Prox1 in the induction of the lymphatic endothelial cell phenotype. *Embo j* 2002;**21**:1505-1513.
51. Seo S, Kume T. Forkhead transcription factors, Foxc1 and Foxc2, are required for the morphogenesis of the cardiac outflow tract. *Developmental Biology* 2006;**296**:421-436.
52. Laforest B, Nemer M. GATA5 interacts with GATA4 and GATA6 in outflow tract development. *Dev Biol* 2011;**358**:368-378.
53. Corada M, Orsenigo F, Morini MF, Pitulescu ME, Bhat G, Nyqvist D, Breviario F, Conti V, Briot A, Iruela-Arispe ML, Adams RH, Dejana E. Sox17 is indispensable for acquisition and maintenance of arterial identity. *Nat Commun* 2013;**4**:2609.
54. Lupu I-E, De Val S, Smart N. Coronary vessel formation in development and disease: mechanisms and insights for therapy. *Nature Reviews Cardiology* 2020;**17**:790-806.
55. Chen HI, Sharma B, Akerberg BN, Numi HJ, Kivelä R, Saharinen P, Aghajanian H, McKay AS, Bogard PE, Chang AH, Jacobs AH, Epstein JA, Stankunas K, Alitalo K, Red-Horse K. The sinus venosus contributes to coronary vasculature through VEGFC-stimulated angiogenesis. *Development* 2014;**141**:4500-4512.
56. Sharma B, Ho L, Ford GH, Chen HI, Goldstone AB, Woo YJ, Quertermous T, Reversade B, Red-Horse K. Alternative Progenitor Cells Compensate to Rebuild the Coronary Vasculature in Elabela- and Apj-Deficient Hearts. *Developmental Cell* 2017;**42**:655-666.e653.
57. Neal A, Nornes S, Payne S, Wallace MD, Fritzsche M, Louphrasitthiphol P, Wilkinson RN, Chouliaras KM, Liu K, Plant K, Sholapurkar R, Ratnayaka I, Herzog W, Bond G, Chico T, Bou-Gharios G, De Val S. Venous identity requires BMP signalling through ALK3. *Nat Commun* 2019;**10**:453.
58. D'Amato G, Phansalkar R, Naftaly JA, Rios Coronado PE, Cowley DO, Quinn KE, Sharma B, Caron KM, Vigilante A, Red-Horse K. Endocardium-to-coronary artery differentiation during heart development and regeneration involves sequential roles of Bmp2 and Cxcl12/Cxcr4. *bioRxiv* 2021:2021.2010.2025.465773.
59. Vanlandewijck M, He L, Mäe MA, Andrae J, Ando K, Del Gaudio F, Nahar K, Lebouvier T, Laviña B, Gouveia L, Sun Y, Raschperger E, Räsänen M, Zarb Y, Mochizuki N, Keller

A, Lendahl U, Betsholtz C. A molecular atlas of cell types and zonation in the brain vasculature. *Nature* 2018;**554**:475-480.

60. Park SM, Angel CE, McIntosh JD, Mansell C, Chen CJ, Cebon J, Dunbar PR. Mapping the distinctive populations of lymphatic endothelial cells in different zones of human lymph nodes. *PLoS One* 2014;**9**:e94781.
61. Kilic N, Oliveira-Ferrer L, Neshat-Vahid S, Irmak S, Obst-Pernberg K, Wurmbach JH, Loges S, Kilic E, Weil J, Lauke H, Tilki D, Singer BB, Ergün S. Lymphatic reprogramming of microvascular endothelial cells by CEA-related cell adhesion molecule-1 via interaction with VEGFR-3 and Prox1. *Blood* 2007;**110**:4223-4233.
62. Deng Y, Larrivée B, Zhuang ZW, Atri D, Moraes F, Prahst C, Eichmann A, Simons M. Endothelial RAF1/ERK activation regulates arterial morphogenesis. *Blood* 2013;**121**:3988-3996.
63. Hong CC, Peterson QP, Hong J-Y, Peterson RT. Artery/Vein Specification Is Governed by Opposing Phosphatidylinositol-3 Kinase and MAP Kinase/ERK Signaling. *Current Biology* 2006;**16**:1366-1372.
64. Kim KL, Seo S, Kim JT, Kim J, Kim W, Yeo Y, Sung JH, Park SG, Suh W. SCF (Stem Cell Factor) and cKIT Modulate Pathological Ocular Neovascularization. *Arterioscler Thromb Vasc Biol* 2019;**39**:2120-2131.
65. Icli B, Wara AK, Moslehi J, Sun X, Plovie E, Cahill M, Marchini JF, Schissler A, Padera RF, Shi J, Cheng HW, Raghuram S, Arany Z, Liao R, Croce K, MacRae C, Feinberg MW. MicroRNA-26a regulates pathological and physiological angiogenesis by targeting BMP/SMAD1 signaling. *Circ Res* 2013;**113**:1231-1241.
66. Tian X, Hu T, Zhang H, He L, Huang X, Liu Q, Yu W, He L, Yang Z, Yan Y, Yang X, Zhong TP, Pu WT, Zhou B. De novo formation of a distinct coronary vascular population in neonatal heart. *Science* 2014;**345**:90.
67. Lu P, Wang Y, Liu Y, Wu B, Zheng D, Harvey RP, Zhou B. Perinatal angiogenesis from pre-existing coronary vessels via DLL4-NOTCH1 signalling. *Nat Cell Biol* 2021;**23**:967-977.
68. Li Y, Cheng CN, Verdun VA, Wingert RA. Zebrafish nephrogenesis is regulated by interactions between retinoic acid, mecom, and Notch signaling. *Dev Biol* 2014;**386**:111-122.
69. Goyama S, Yamamoto G, Shimabe M, Sato T, Ichikawa M, Ogawa S, Chiba S, Kurokawa M. Evi-1 is a critical regulator for hematopoietic stem cells and transformed leukemic cells. *Cell Stem Cell* 2008;**3**:207-220.
70. Swift MR, Pham VN, Castranova D, Bell K, Poole RJ, Weinstein BM. SoxF factors and Notch regulate nr2f2 gene expression during venous differentiation in zebrafish. *Developmental Biology* 2014;**390**:116-125.
71. Wolf K, Hu H, Isaji T, Dardik A. Molecular identity of arteries, veins, and lymphatics. *Journal of Vascular Surgery* 2019;**69**:253-262.

Figure Legends

Figure 1: Mapping the human fetal heart endothelium using scRNA-seq.

(A) Schematic of experimental design for mapping the human fetal heart endothelium using 10X scRNA-seq. **(B)** Representative FACS gating strategy used to isolate viable CD31+ CD45- endothelial cells. **(C)** UMAP visualisation of clusters identified in scRNA-seq data from cardiac endothelial cells isolated from human fetal heart (n=2). **(D)** Feature plots showing expression of key marker genes defining distinct endothelial populations. **(E)** Metagene analysis of fetal heart scRNA-seq data visualised in self organised maps for total dataset (left) and subpopulations of endothelial cell (right). Radar plots show enrichment of each metagene signature in individual clusters. **(F)** GO term enrichment analysis conducted using genes from metagenes' signatures A (left) and F (right).

Figure 2: Gene regulatory network analysis of human fetal heart endothelium.

(A) Heatmap of differentially expressed cluster genes: expression of top 20 differentially expressed genes for each cluster identified in the complete dataset. Genes were grouped according to the cluster in which they were differentially expressed. **(B)** Violin plots: expression of *CD36, RGCC, INMT*, and *KIT* across clusters identified in fetal heart endothelial cell dataset. **(C)** Gene regulatory network constructed using SCENIC analysis. Transcription factors and target genes shown as squares or circles, respectively. Genes are coloured based on the cluster in which they were differentially expressed. White nodes represent gene targets that were not differentially expressed. **(D)** Violin plots showing enrichment/AUC score of *SOX4* and *SMAD1* regulons across identified clusters.

Figure 3: Trajectory inference analysis of developing cardiac endothelium.

(A) RNA velocity analysis of microvascular cardiac endothelium. The RNA velocity field shown superimposed onto a UMAP visualisation of microvascular cardiac endothelial cells. **(B)** Slingshot trajectory demonstrating pseudotemporal cellular dynamics. **(C)** Heatmap of 200 genes found to be most differentially expressed across pseudotime of trajectory from Panel B. Genes grouped into modules by k-means clustering (k=4). **(D)** Smoothing spline curves show average sample scaled gene expression for genes within modules identified in Panel A. **(E)** Feature plots showing expression of selected genes from modules 2 (*DKK3* and *GATA6*), 3 (*MECOM* and *HEY1*), or 4 (*TCF15* and *MEOX1*). **(F)** In situ hybridisation validation of co-expression of *MECOM* (green) with HEY1 (red) in arterial EC of a 13-week human fetal heart (sample #1). See supplementary Figure 5A for samples #2, #3, and #4. A = artery, V = vein.

Figure 4: Comparison of the transcriptional profiles of human and mouse fetal cardiac endothelial cell populations.

(A) Heatmaps showing expression of either conserved (left) or human-specific (right) markers for each subpopulation of fetal cardiac endothelium. **(B)** Expression of selected conserved markers in EC populations in human and mouse. **(C)** Expression of markers identified as being human-specific.

Figure 5: Knockdown of MECOM in hESC-EC.

(A) Experimental design for siRNA mediated knockdown of MECOM in hESC-EC. **(B)** Quantification of MECOM protein abundance following siRNA knockdown using siRNA MECOM 1 (n = 4 biological replicates) and siRNA MECOM 2 (n = 3 biological replicates). P-values were obtained using an unpaired t-test. **(C)** Volcano plot showing differential gene

expression following MECOM siRNA-mediated knockdown in hESC-EC (n = 4 biological replicates). P-values calculated using the Wald test. **(D)** Upregulated gene signature score applied across identified clusters in fetal heart EC scRNA-seq dataset. Upregulated gene signature constructed using top 20 genes found to be significantly upregulated following MECOM knockdown in hESC-EC. **(E)** KEGG pathway enrichment analysis conducted using significantly upregulated genes following MECOM knockdown. **(F)** qRT-PCR quantification of known markers of arterial (*DLL4*, *HEY1*) and venous (*EPHB4, NR2F2*) EC after MECOM siRNA knockdown (n = 4 biological replicates). P-values were calculated using a one-way ANOVA followed by Dunnett's post-hoc multiple comparison test. Graphs in panels B and F correspond to mean ± standard error of the mean.

Figure 1.

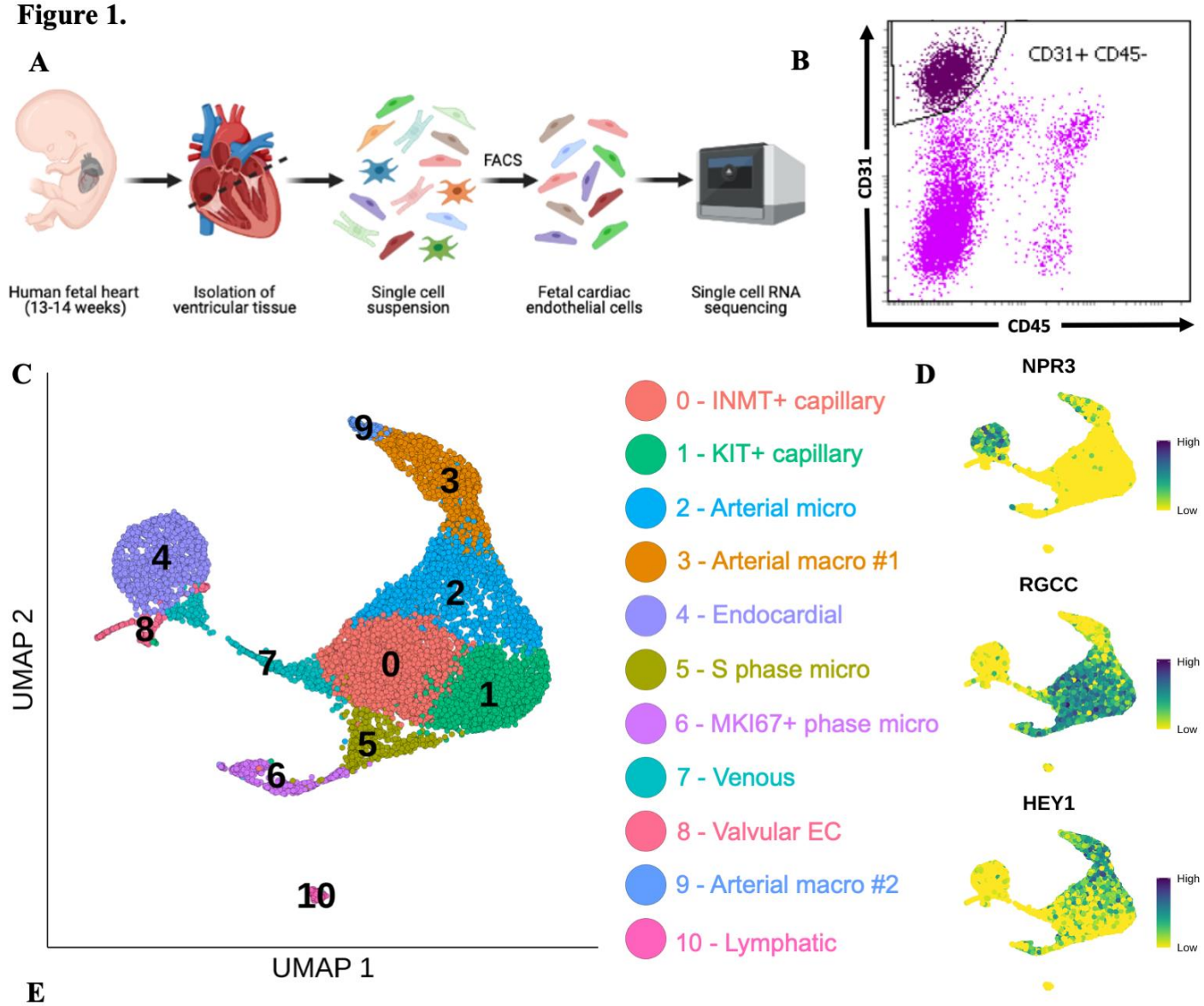

Figure 2.

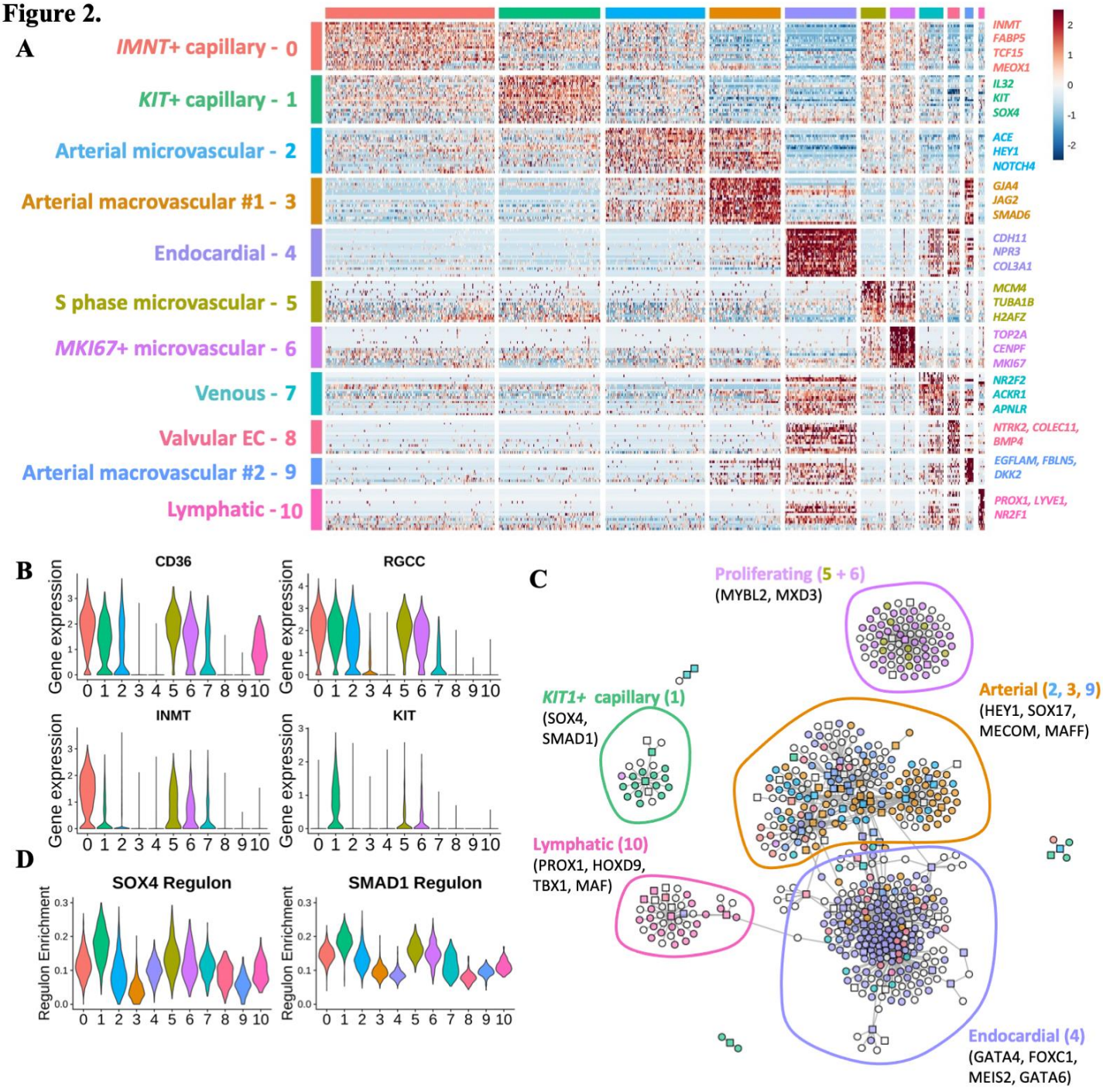

Figure 3.

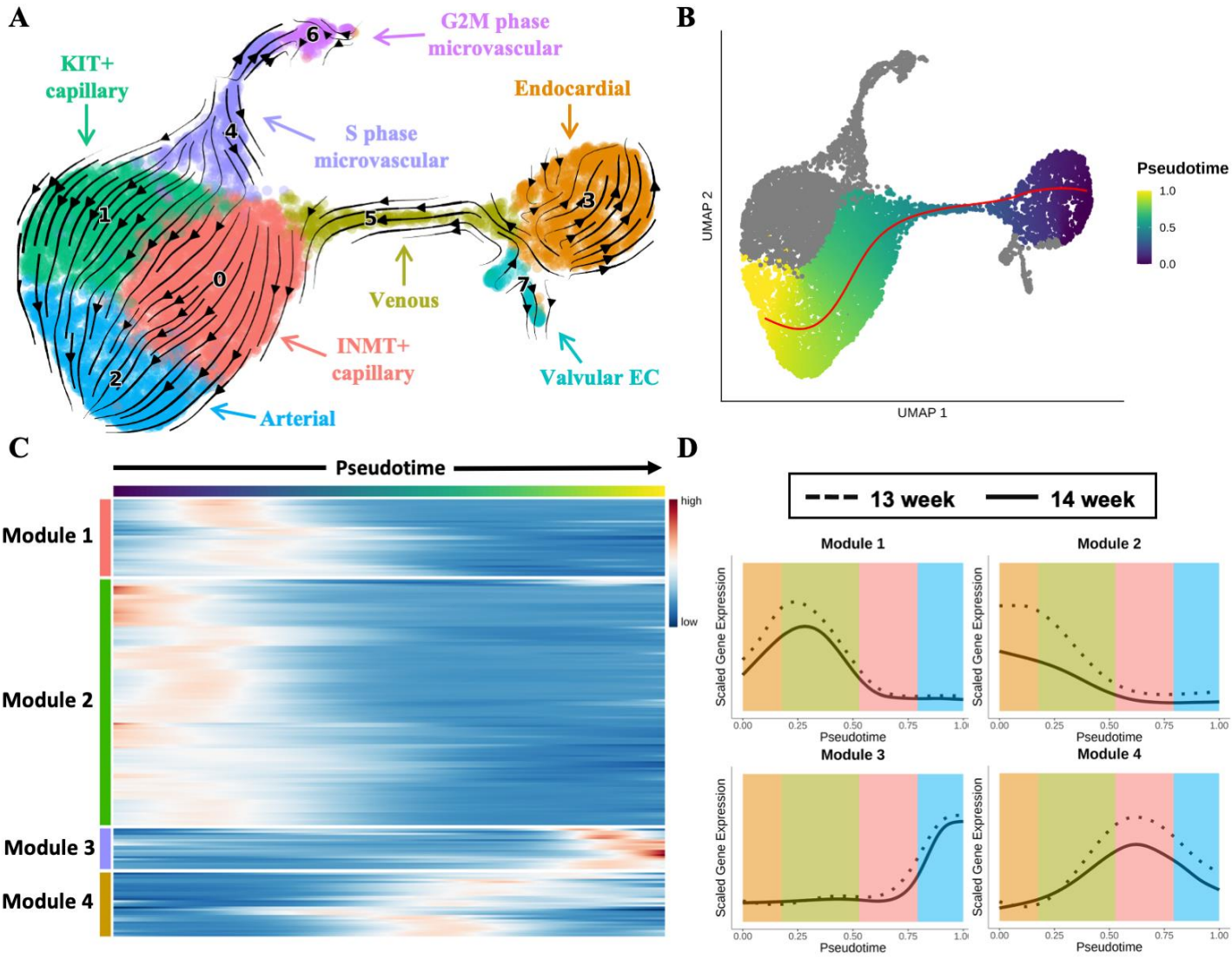

Figure 4.

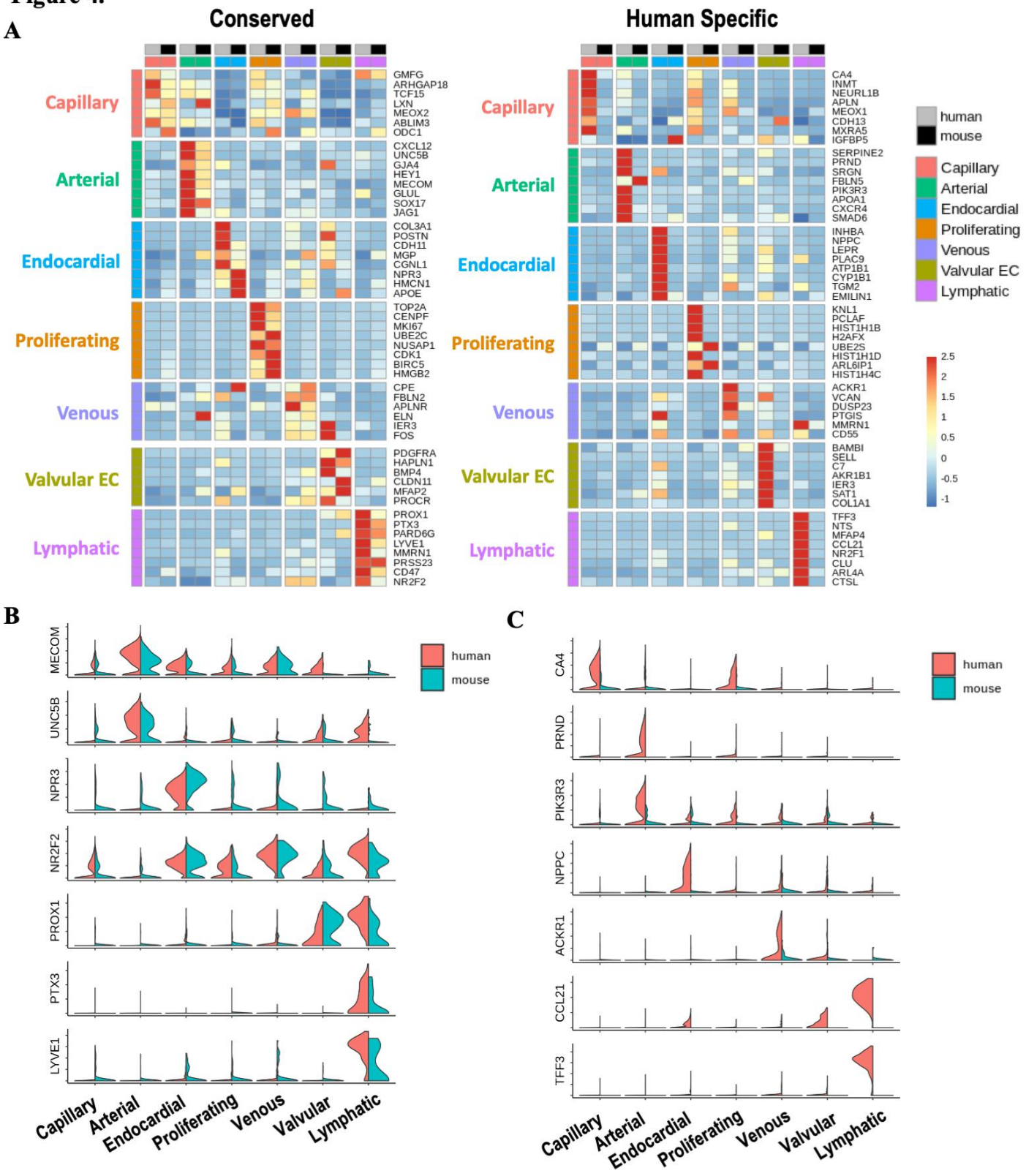

Figure 5.

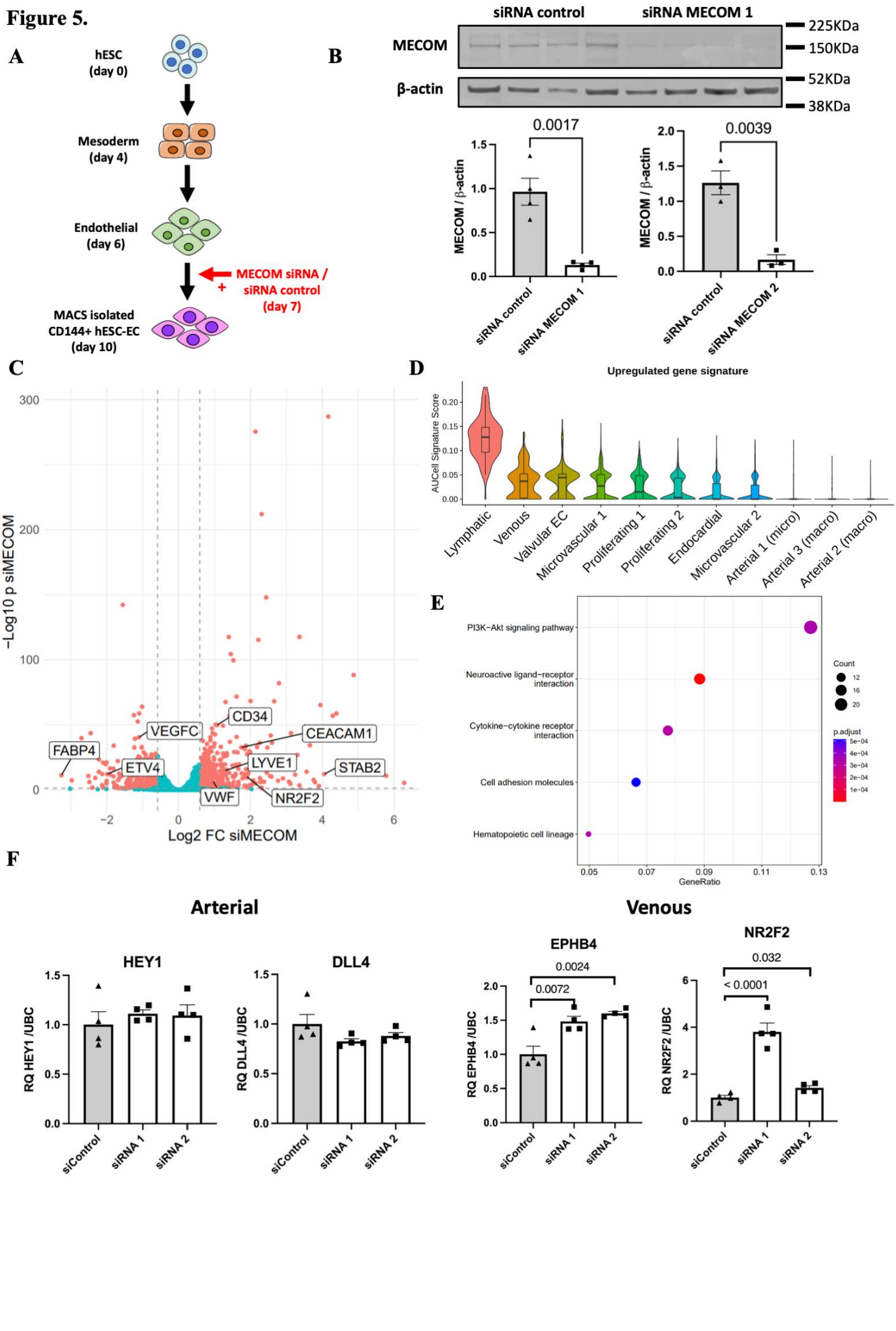

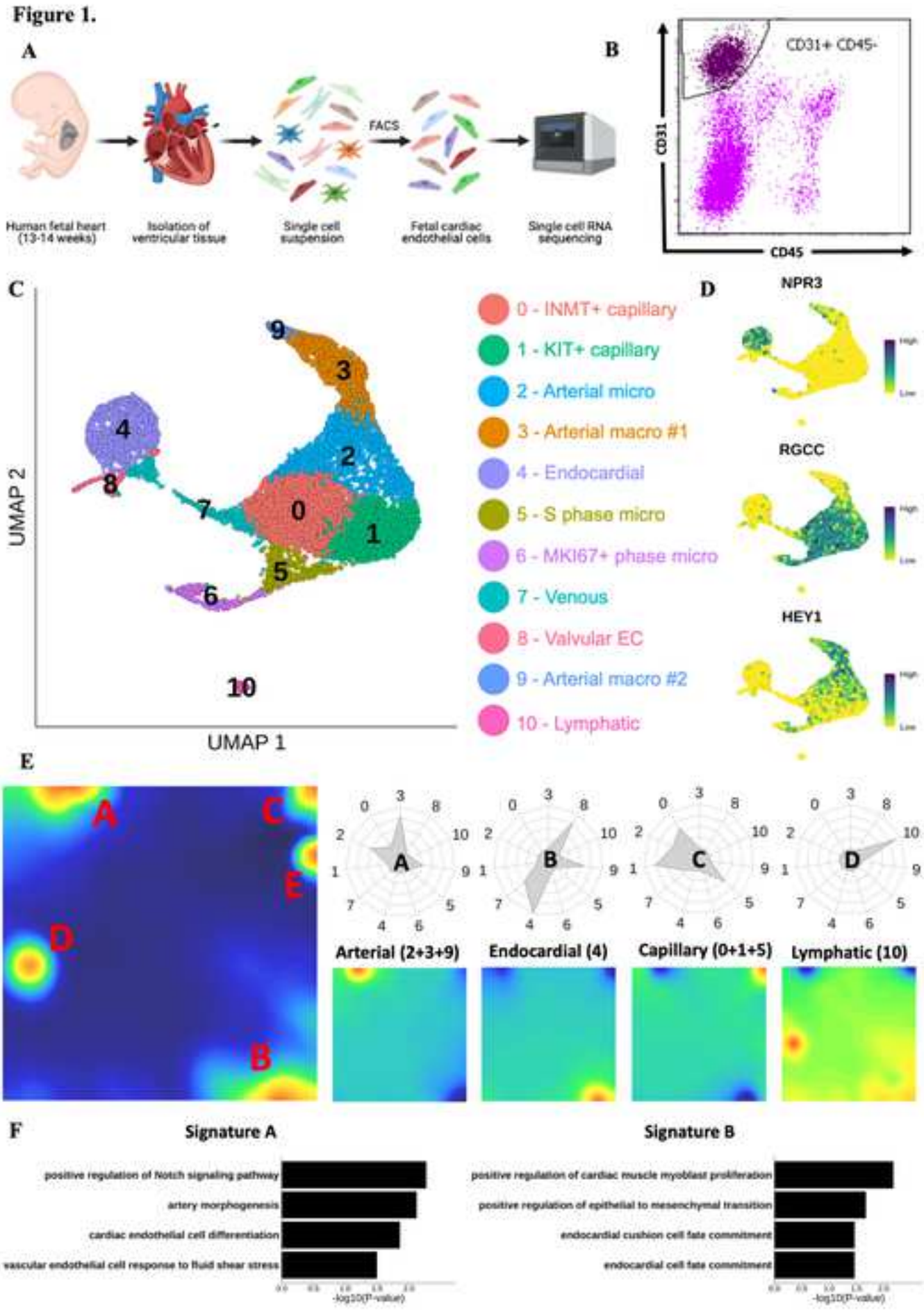

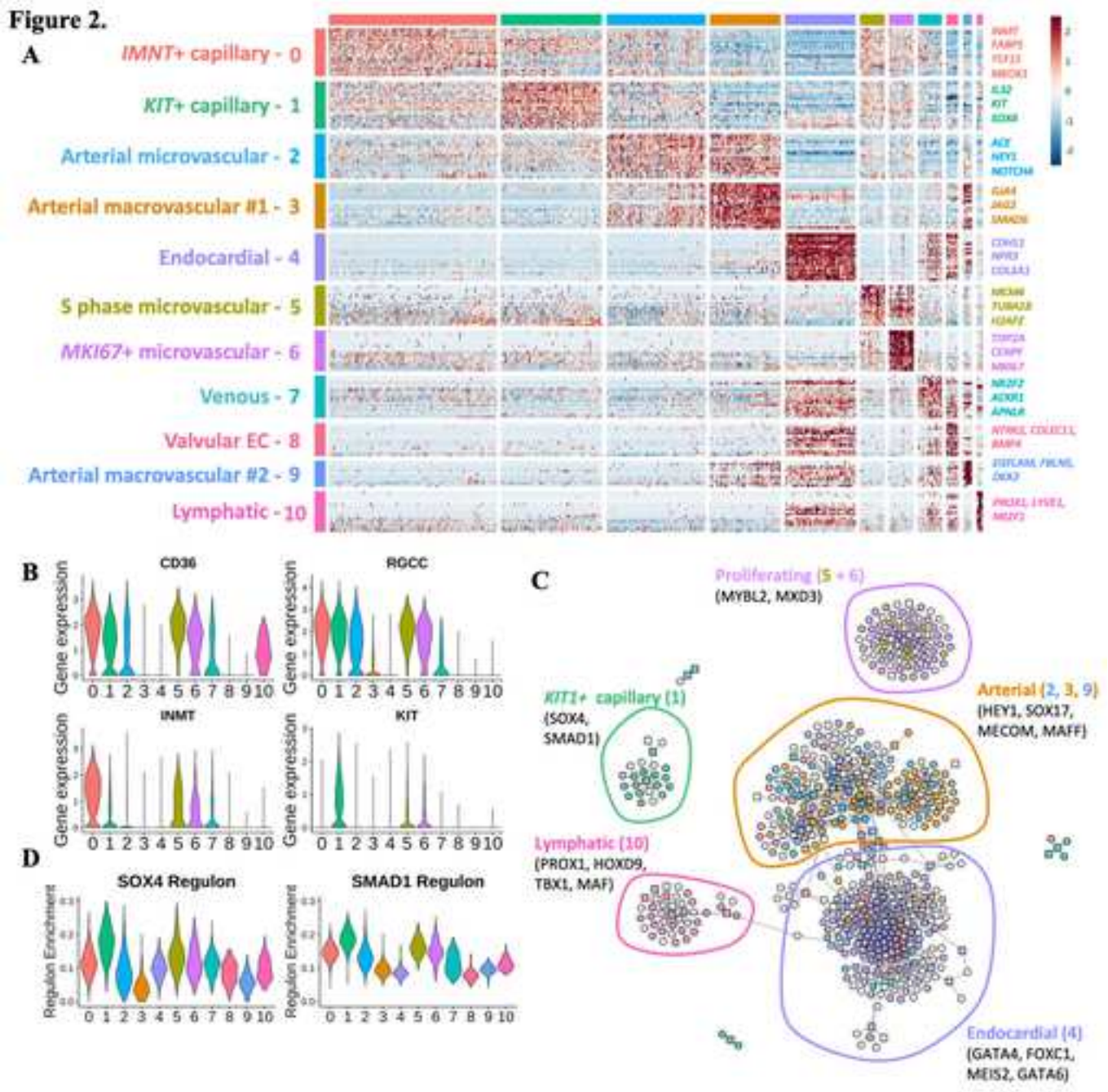

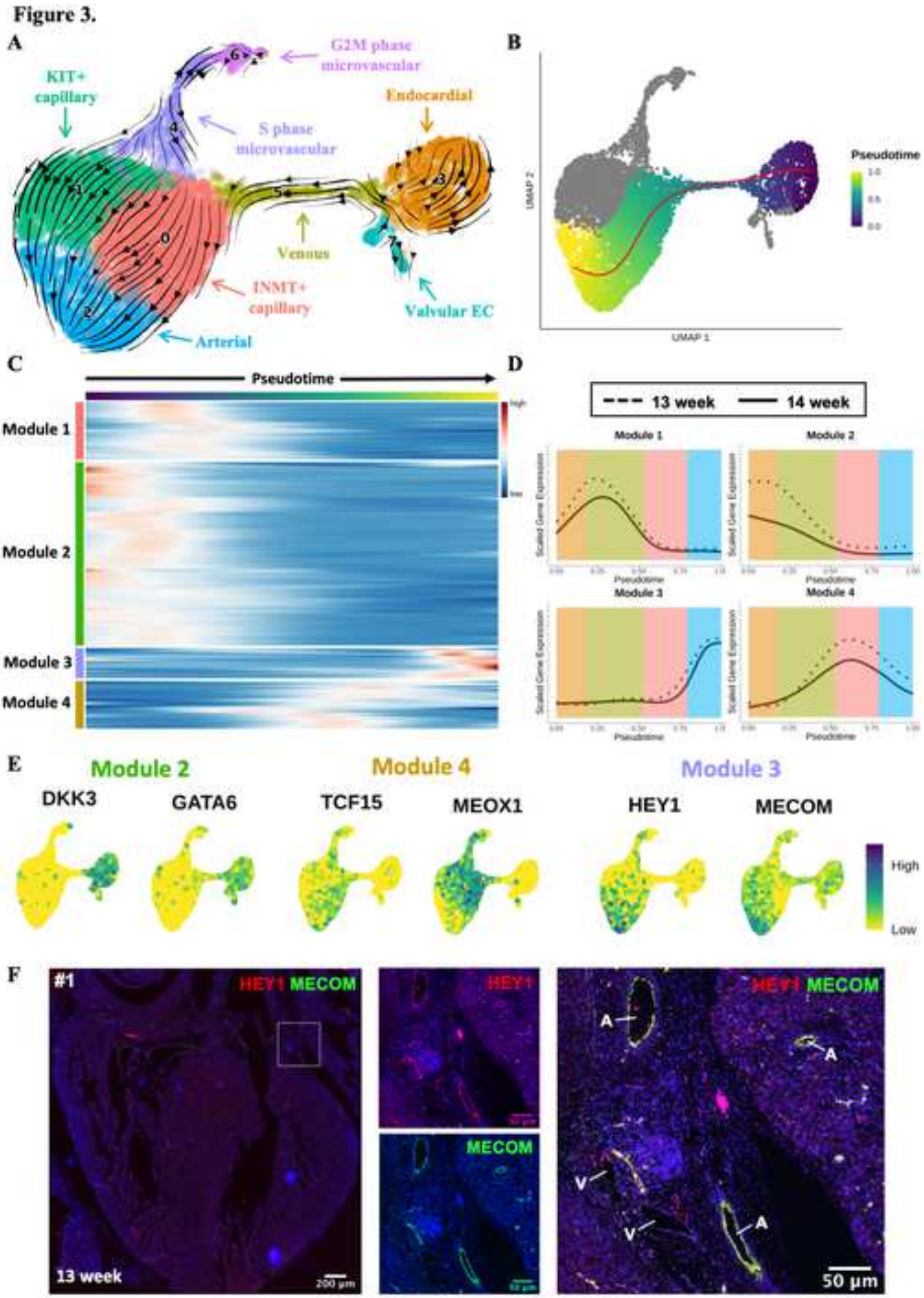

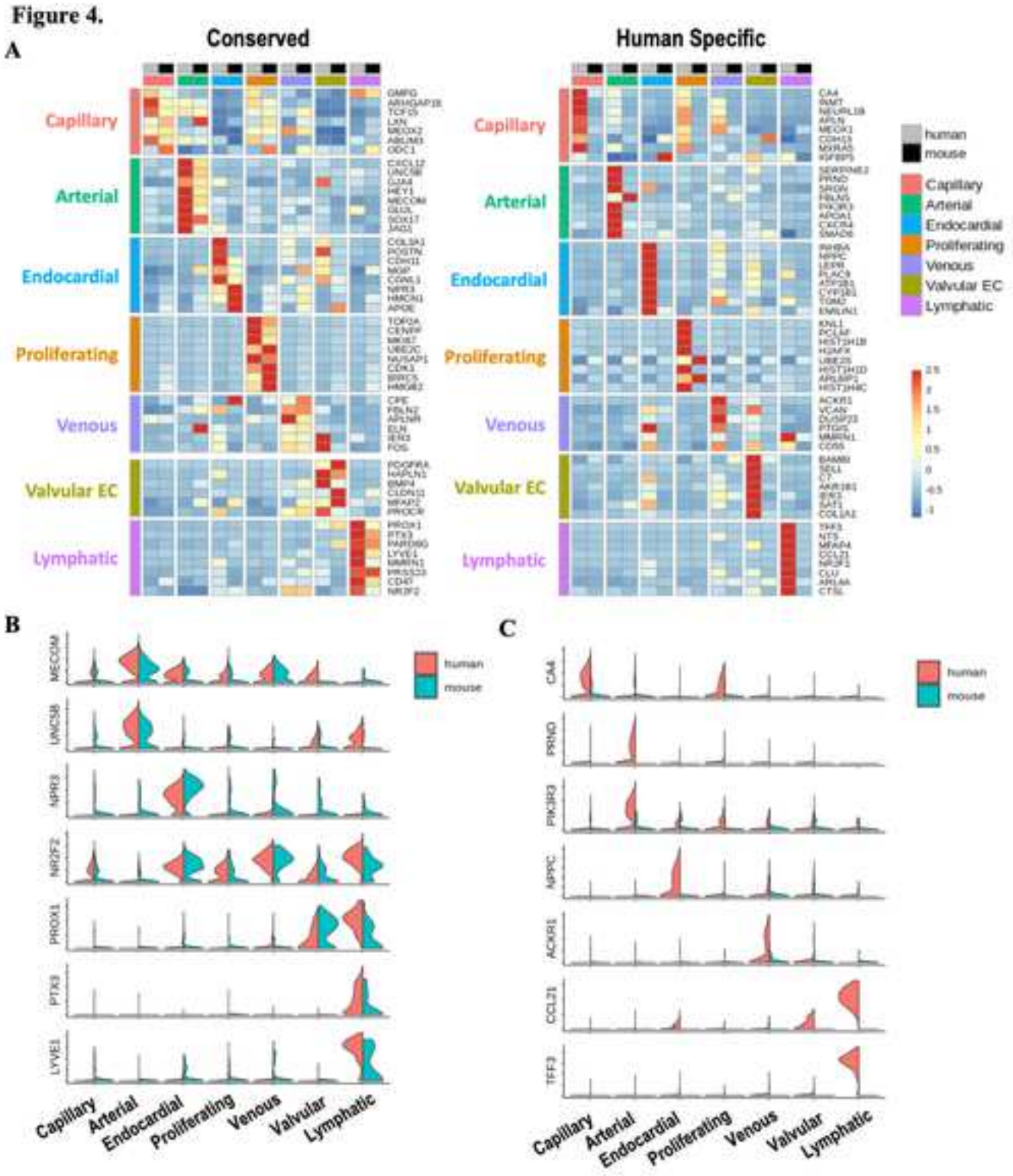

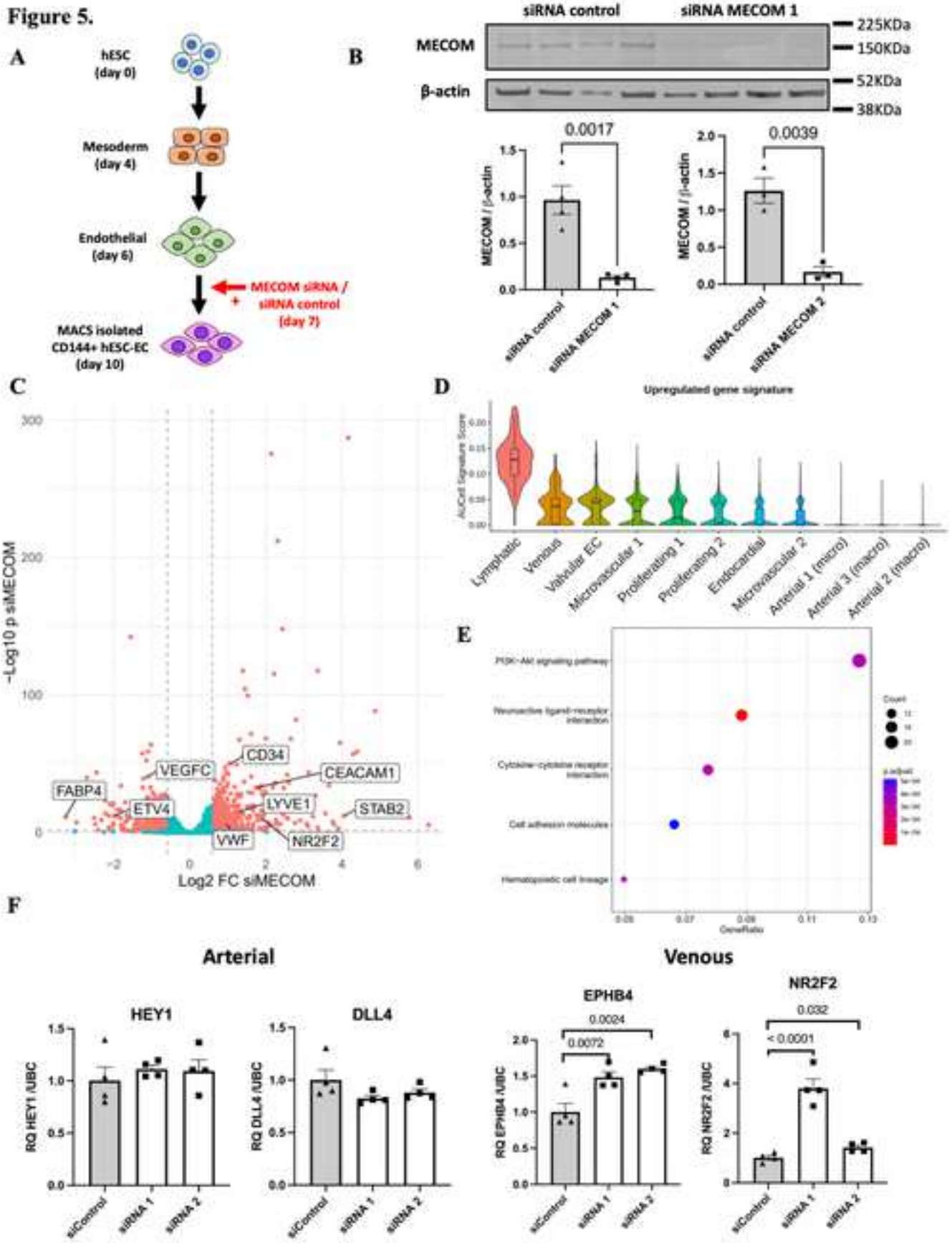

Graphical Abstract